

Ellipsotopes: Combining Ellipsoids and Zonotopes for Reachability Analysis and Fault Detection

Shreyas Kousik¹, Adam Dai² and Grace X. Gao¹

Abstract—Ellipsoids are a common representation for reachability analysis because they are closed under affine maps and allow conservative approximation of Minkowski sums; this enables one to incorporate uncertainty and linearization error in a dynamical system by expanding the size of the reachable set. Zonotopes, a type of symmetric, convex polytope, are similarly frequently used due to efficient numerical implementation of affine maps and exact Minkowski sums. Both of these representations also enable efficient, convex collision detection for fault detection or formal verification tasks, wherein one checks if the reachable set of a system collides (i.e., intersects) with an unsafe set. However, both representations often result in conservative representations for reachable sets of arbitrary systems, and neither is closed under intersection. Recently, constrained zonotopes and constrained polynomial zonotopes have been shown to overcome some of these conservatism challenges, and are closed under intersection. However, constrained zonotopes can not represent shapes with smooth boundaries such as ellipsoids, and constrained polynomial zonotopes can require solving a non-convex program for collision checking (i.e., fault detection). This paper introduces *ellipsotopes*, a set representation that is closed under affine maps, Minkowski sums, and intersections. Ellipsotopes combine the advantages of ellipsoids and zonotopes, and enable convex collision checking at the expense of more conservative reachable sets than constrained polynomial zonotopes. The utility of this representation is demonstrated on several examples.

I. INTRODUCTION

In the controls, robotics, and navigation communities, it is often critical to place strict guarantees on the behavior of a dynamical system. Example applications of such guarantees include collision avoidance [1]–[4], fault detection [5], [6], and control invariance [4], [7], [8]. A common strategy for enforcing such guarantees, especially for uncertain dynamical systems, is to compute the system’s reachable set of states, then guarantee that this set lies within certain bounds (e.g., for fault detection) or obeys non-intersection constraints (e.g., for collision avoidance).

Directly representing a continuum of possible system trajectories numerically is typically intractable, given that these trajectories are solutions to a nonlinear differential or difference equation. Instead, a variety of set representations have been introduced to enable approximating reachable sets. Two of the most common and well-studied representations are ellipsoids [9], [10] and zonotopes [2], [11], [12]. In this work, an ellipsoid is best understood as an affine transformation of a unit 2-norm ball in an arbitrary-dimensional Euclidean space. A zonotope can similarly be understood as

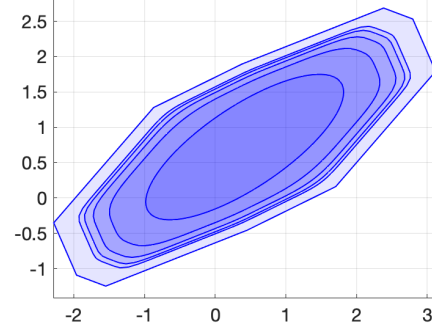


Fig. 1: Basic ellipsotopes with five generators and increasing p -norm ($p = 2, 4, \dots, 10$), shown with lighter blue as the norm increases. The outermost shape is the ∞ -norm zonotope, and the innermost shape is the 2-norm ellipsoid.

the affine transformation of the unit ∞ -norm ball, resulting in a symmetric polytope. We propose a novel set representation, *ellipsotopes*, by generalizing to arbitrary p -norms, as shown in Fig. 1.

A. Ellipsoids and Zonotopes

Both ellipsoids and zonotopes provide straightforward numerical implementations of operations that are commonly-used for reachability analysis, fault detection, and similar tasks. For example, both representations can be transformed readily via affine maps, thereby representing the flow of a (linearized) dynamical system. Furthermore, one can apply convex programming to efficiently detect when these sets intersect with e.g., obstacles for collision avoidance [6], [10], [13]. However, choosing between the two representations comes with certain tradeoffs. For example, zonotopes are closed under Minkowski sums, which are used to incorporate uncertainty and linearization error, while ellipsoids are not. On the other hand, ellipsoids can exactly represent the confidence level sets of Gaussian distributions, while zonotopes cannot.

Note, we present a more detailed discussion of other set representations, both convex and non-convex, in Section II. Out of the convex representations, we consider ellipsoids and zonotopes the best-suited for reachability and fault detection tasks. For the non-convex representations, we typically lose the ability to perform efficient, convex collision-checking.

B. Contributions

Our main contribution is a novel set representation called the *ellipsotope*, which combines the advantages of both ellip-

¹ Aeronautics and Astronautics, Stanford University, Stanford, CA.

² Electrical Engineering, Stanford University, Stanford, CA.

Corresponding author: gracegao@stanford.edu.

soids and zonotopes. For the purposes of reachability analysis and fault detection, we show that ellipsotopes are closed under linear maps, Minkowski sums, and intersections. We also introduce several order reduction strategies for managing ellipsotope complexity, which can grow during reachability analysis. We demonstrate the utility of these objects with a variety of numerical examples.

C. Paper Organization

Section II discusses a variety of set representations to clarify the context for ellipsotopes. Section III introduces notation and set representations relevant to developing ellipsotopes. Section IV defines ellipsotopes and discusses properties and closed operations. Section V covers methods for order reduction. Section VI covers numerical examples and applications of ellipsotopes. Section VII concludes the paper.

II. RELATED WORK

A variety of set representations exist for reachability analysis and fault detection. We now discuss these representations, and under which operations they are *closed*, meaning that an operation yields an instance of the same representation. We divide our discussion by convex and non-convex sets.

A. Convex Set Representations

Convex representations enable one to use convex programming to evaluate intersection and set membership. This enables one to certify that, e.g., a system’s reachable set lies within a safe region, because a convex program is guaranteed to converge. In particular, we discuss ellipsoids, convex polytopes, and support functions.

As mentioned before, ellipsoids are affine transformations of the 2-norm ball. This set representation is closed under affine transformations and hyperplane intersections [9]. For operations such as Minkowski sum, intersection, Pontryagin (Minkowski) difference, and convex hull, efficient algorithms exist to generate inner- and outerapproximative ellipsoids [10], [14], [15]. Most importantly, for tasks such as reachability analysis, confidence level sets of multivariate Gaussian distributions are ellipsoidal. Unfortunately, ellipsoidal representations of reachable sets can rapidly become conservative due to the overapproximation required for Minkowski sums. Furthermore, ellipsoids are not well-suited to representing polytopic sets such as occupancy grids, which are commonly used for tasks such as robot motion planning.

Convex polytopes can be thought of as the bounded intersection of a collection of affine halfspaces in arbitrary dimensions (H-representation); note, an unbounded intersection is called a polyhedron [16]. Another common representation is as the convex hull of a set of vertices (V-representation). This broad category of objects is closed under Minkowski sum, intersection, Pontryagin difference, and convex hull [17]. The H-representation is especially convenient for determining if a polytope contains a point and performing intersections. However, the remaining operations are not computationally

efficient, especially in high dimensions or when a convex polytope is defined by a large number of halfspaces.

To avoid these challenges, zonotopes have become a popular representation that enable efficient Minkowski sums and set containment queries [2], [11]–[13], [16]. A zonotope is a centrally-symmetric convex polytope constructed as a Minkowski sum of line segments. Zonotopes can be parameterized by a center and generator (see (2) in Section III), which we call a CG-representation; any point in the zonotope is the center plus a linear combination of the generators, each scaled by a coefficient in $[-1, 1]$. Since zonotopes are not closed under intersection or Pontryagin difference, several authors have introduced AH-polytopes [16] and constrained zonotopes [6]. An AH-polytope is the affine transformation of an H-representation of a polytope (e.g., a zonotope is the affine transformation of a hypercube). A constrained zonotope is a zonotope with additional linear constraints on its coefficients. These representations are closed under affine transformation, Minkowski sum, intersection, and, for constrained zonotopes, Pontryagin difference and convex hull [18]. All convex polytopes are constrained zonotopes, and set membership or intersection queries can be evaluated by solving a linear program [6]. While AH-polytopes and constrained zonotopes overcome many of the challenges of zonotopes, they still cannot represent sets with smooth curved boundaries, such as ellipsoids.

Support functions enable one to represent arbitrary convex sets, allowing generalization beyond polytopes and ellipsoids [19]–[21]. A support function is a convex function that maps a vector in Euclidean space to the maximum dot product between that vector and any element in a convex set, thereby providing an implicit set representation. Support functions of many convex sets, such as unit balls, ellipsoids, and zonotopes, have a simple analytical form, and the support function for polytopes can be expressed as the solution of a linear program [20]. Furthermore, affine maps, Minkowski sums, and convex hulls have analytic formulations. Unfortunately, the intersection of sets represented by support functions can only be overapproximated and results in a non-convex representation [21, Prop. 4], so using intersection for collision-checking and fault detection is neither straightforward nor conservative.

B. Non-Convex Set Representations

The reachable set of a dynamical system is not necessarily convex. Furthermore, robots and other autonomous systems frequently have non-convex bodies, and such systems are not necessarily subject to convex constraints for fault detection or collision avoidance. A variety of non-convex set representations exist that attempt to address these challenges. In particular, we discuss polynomial zonotopes, star sets, level sets, and Constructive Solid Geometry (CSG).

Polynomial zonotopes (PZs) are a generalization of zonotopes wherein the coefficients of a zonotope’s generators are instead allowed to be monomials [22], [23]. By leveraging the center/generator structure of zonotopes, these sets are closed under affine transformation and Minkowski sum. One

can add polynomial constraints on the coefficients to make constrained polynomial zonotopes (CPZs), which are closed under intersection and convex hull [24]. PZs and CPZs provide much tighter (i.e., less conservative) approximations of reachable sets than zonotopes, at the expense of being non-convex. This means that collision checking requires solving a non-convex program, typically preventing solution guarantees. One alternative is to overapproximate a PZ or CPZ with a zonotope [25], resulting in a convex collision check at the expense of significant increase in conservatism.

Star sets are also a generalization of zonotopes and ellipsoids [26]–[28], which instead use a generic logical predicate constraint on their generator coefficients. These sets can be non-convex, and are closed under affine transformation, Minkowski sum, and intersection. However, similar to PZs and CPZs, checking for emptiness or collision can require solving a non-convex feasibility problem.

Departing from the center/generator construction used for zonotopes and similar objects, level sets are a popular representation for reachability analysis, because arbitrary sets can be represented as the 0-sublevel set of a function. Such a function can be approximated on a grid [29], [30] or as a polynomial [31]. Level sets can be used to conservatively compute reachable sets of robots and similar systems subject to uncertainty [1], [4], [32], [33]. In the special case of rigid-body robot motion planning with polynomial level sets, one can represent collision checking as a polynomial evaluation [1]; however, in general, Minkowski sums, intersections, and convex hulls can be approximated using sums-of-squares programming. Level set methods typically do not require linear maps and Minkowski sums to perform reachability analysis; however, they instead require approximately solving either the Hamilton-Jacobi-Bellman or Liouville partial differential equations. Furthermore, level set representations suffer from the curse of dimensionality, requiring decompositions or approximations for nonlinear dynamical systems with more than 5 dimensions [1], [4].

The final set representation we discuss is Constructive Solid Geometry (CSG), which is used to model non-convex shapes in the computer graphics community [34], [35]. Similar to support functions, CSG leverages an implicit point membership classification function to express geometric primitives such as spheres, prisms, and cones. Non-convex bodies are represented as unions, intersections, and set differences of the primitives, which can also be approximated with smooth functions [36]. This representation has been applied to reachability analysis, with similar advantages and drawbacks as we see for support functions [36], [37]. For these sets, computing Minkowski sums is challenging; furthermore, these representations are typically limited to 2-D or 3-D settings, and it is unclear how to reduce the growing complexity of a reachable set in a similar way to zonotope order reduction.

C. Summary

From this review of a wide variety of representations, we identify several advantages and challenges. The advantages

of zonotopes and similar objects is their numerical simplicity for representing affine transformations, Minkowski sums, and collision/emptiness checking (via intersection operations). The challenges are to represent smooth or non-polytopic sets without incurring conservatism (as with ellipsoids) or non-convexity (as with polynomial zonotopes). Our proposed ellipsotope representation directly addresses this tradeoff by enabling efficient reachability and fault detection operations for both polytope-like and ellipsoid-like objects without introducing challenges from losing convexity.

III. PRELIMINARIES

We now introduce notation and several set representations.

A. Notation

1) *Points, Sets, and Set Operations*: Scalars and vectors are lowercase and italic. Sets and matrices are uppercase italic. The real numbers are \mathbb{R} , and the natural numbers are \mathbb{N} . If $n \in \mathbb{N}$, we denote $\mathbb{N}_n = \{1, 2, \dots, n\} \subset \mathbb{N}$. The p -norm unit ball in \mathbb{R}^n is $\mathcal{B}_{p,n} = \{x \in \mathbb{R}^n \mid \|x\|_p \leq 1\}$. An affine subspace (i.e., affine hyperplane) of \mathbb{R}^n parameterized by $H \in \mathbb{R}^{n \times m}$, $m \in \mathbb{N}$, and $f \in \mathbb{R}^m$ is $\mathcal{P}(H, f) = \{x \in \mathbb{R}^n \mid Hx = f\}$. A halfspace parameterized by $h \in \mathbb{R}^n$ and $s \in \mathbb{R}$ is $\mathcal{H}(h, s) = \{x \in \mathbb{R}^n \mid h^\top x \leq s\}$.

Let A be a set such that $A \subset \mathbb{R}^n$. Its power set is $\text{pow}(A)$, its cardinality is $|A|$, and its boundary is $\text{bd}(A)$. Let $B \subset \mathbb{R}^n$ as well. The Minkowski sum is $A \oplus B = \{a + b \mid a \in A, b \in B\}$. The convex hull of $A \cup B$ is $\text{CH}(A \cup B) = \{\lambda a + (1 - \lambda)b \mid \lambda \in [0, 1], a \in A, b \in B\}$.

Consider a set of integers $J = \{j_1, j_2, \dots, j_n\} \subset \mathbb{N}$ and $m \in \mathbb{N}$; then $J + m = \{j_1 + m, \dots, j_n + m\}$. Similarly, consider a set of sets of integers $\mathcal{J} = \{J_1, J_2, \dots, J_n\} \subset \text{pow}(\mathbb{N})$. We denote $\mathcal{J} + m$ to mean $\{J_1 + m, J_2 + m, \dots, J_n + m\}$.

2) *Vectors, Arrays, and Matrices*: An $n \times m$ matrix of ones is $1_{n \times m}$. Similarly, a matrix of zeros is $0_{n \times m}$. An $n \times n$ identity matrix is I_n . Let $v \in \mathbb{R}^n, w \in \mathbb{R}^m$; we denote vector concatenation by $(v, w) \in \mathbb{R}^{n+m}$. The $\text{diag}(\cdot)$ operator places its arguments (block) diagonally on a matrix of zeros. The $\text{eig}(\cdot)$ operator returns a column vector containing the eigenvalues of its input matrix. The $\text{det}(A)$ operator returns the determinant of a square matrix A .

Let $v \in \mathbb{R}^n$ and $J \subset \mathbb{N}_n$. Then $v\langle J \rangle \in \mathbb{R}^{|J|}$ is the vector of elements of v indexed by J . Similarly, if $A \in \mathbb{R}^{n \times m}$, $J_1 \subset \mathbb{N}_n$, and $J_2 \subset \mathbb{N}_m$, then $A\langle J_1, J_2 \rangle$ is the $|J_1| \times |J_2|$ sub-matrix of A . We denote $A\langle J, \cdot \rangle$ as the $|J| \times m$ submatrix of A (that is, the J -rows and all the columns). For a vector $v \in \mathbb{R}^n$ and an integer matrix $M \in \mathbb{N}^{m \times n}$, let $v^M \in \mathbb{R}^m$ denote a vector for which $v^M\langle j \rangle = \prod_{i=1}^n (v\langle i \rangle)^{M\langle j, i \rangle}$ with $j = 1, \dots, m$.

B. Set Representations

An *ellipsoid* is the set

$$\mathcal{E}(c, Q) = \left\{ x \in \mathbb{R}^n \mid (x - c)^\top Q (x - c) \leq 1 \right\}. \quad (1)$$

We call c its *center* and positive definite $Q \succ 0$ its *shape matrix*. Note that one may also see Q^{-1} as defining an ellipsoid [14], [38].

A *zonotope* $\mathcal{Z}(c, G) \subset \mathbb{R}^n$ is a convex, symmetrical polytope parameterized by a *center* $c \in \mathbb{R}^n$ and a *generator matrix* $G \in \mathbb{R}^{n \times m}$, given by

$$\mathcal{Z}(c, G) = \{c + G\beta \mid \|\beta\|_\infty \leq 1\}. \quad (2)$$

That is, a zonotope is a set of convex combinations of c with the columns of the matrix G , which we call *generators*. We call β the generator *coefficients*.

For context, we also provide the definitions for related set representations. From [6], a *constrained zonotope* is defined as follows. Let $A \in \mathbb{R}^{k \times m}$ and $b \in \mathbb{R}^k$, where $k \in \mathbb{N}$ is the number of linear constraints. We denote a constrained zonotope as

$$\mathcal{CZ}(c, G, A, b) = \{c + G\beta \in \mathbb{R}^n \mid \|\beta\|_\infty \leq 1 \text{ and } A\beta = b\}, \quad (3)$$

where c and G are as in (2).

Finally, we introduce *constrained polynomial zonotopes* (CPZs) [24]. Given $c \in \mathbb{R}^n$, $G \in \mathbb{R}^{n \times m}$, $X \in \mathbb{N}^{m \times m}$, $A \in \mathbb{R}^{k \times m}$, $b \in \mathbb{R}^k$, and $D \in \mathbb{N}^{k \times m}$, a CPZ is the set

$$\mathcal{CPZ}(c, G, X, A, b, D) = \left\{ c + G\beta^X \mid \|\beta\|_\infty \leq 1 \text{ and } A\beta^D - b = 0 \right\}. \quad (4)$$

As one would expect, polynomial zonotopes (PZs) are CPZs without constraints. Importantly, PZs and CPZs are not necessarily convex [23], [24].

IV. ELLIPSOTOPES

In this section, we define ellipsotopes, then discuss several useful properties. We then discuss the specific case of ellipsotopes defined using a 2-norm and conclude the section by relating ellipsotopes to other set representations.

A. Definition

To define ellipsotopes, we first introduce *index sets*.

Definition 1. Let $m \in \mathbb{N}$. Let $\mathcal{J} \subset \text{pow}(\mathbb{N}_m)$ be a partition of \mathbb{N}_m . We call \mathcal{J} an *index set*. That is, \mathcal{J} is a set of multi-indices such that $\mathbb{N}_m = \bigcup_{J \in \mathcal{J}} J$ and $J_1 \cap J_2 = \emptyset$ for any $J_1, J_2 \in \mathcal{J}$.

In other words, every integer from 1 to m occurs in exactly one subset $J \in \mathcal{J}$. As an example, for $m = 3$, $\mathcal{J} = \{\{1, 2\}, \{3\}\}$ obeys the definition.

We now define ellipsotopes:

Definition 2. An ellipsotope is a set

$$\mathcal{E}_p(c, G, A, b, \mathcal{J}) = \left\{ c + G\beta \mid \|\beta\langle J \rangle\|_p \leq 1 \forall J \in \mathcal{J} \text{ and } A\beta = b \right\}, \quad (5)$$

A basic *ellipsotope*, $\mathcal{E}_p(c, G)$, has no constraints or index set. A *constrained ellipsotope*, $\mathcal{E}_p(c, G, A, b)$, has no index set. An *indexed ellipsotope*, $\mathcal{E}_p(c, G, \mathcal{J})$, has no constraints.

One can go further and let the different subsets of β be subject to different p -norms, but we have not yet needed this in practice. We call

$$\mathcal{B}_\times(\mathcal{J}) = \left\{ \beta \in \mathbb{R}^m \mid \|\beta\langle J \rangle\|_p \leq 1 \forall J \in \mathcal{J} \right\} \quad (6)$$

a *ball product* because it is the Cartesian product of $|\mathcal{J}| \in \mathbb{N}$ p -norm balls in the varying dimensions indexed by each $J \in \mathcal{J}$.

B. Operations on Ellipsotopes

Affine maps, Minkowski sums, intersections, and convex emptiness checking are the key operations that make constrained zonotopes and similar set representations useful for tasks such as reachability analysis and fault detection. We now show that ellipsotopes are closed under these operations, and that we can overapproximate the convex hull of a pair of ellipsotopes. We then demonstrate how to check whether or not an ellipsotope is empty, as well as whether or not it contains a particular point, using a convex program. These operations are useful for collision checking an ellipsotope reachable set or detecting faults, as we show in Sec. VI.

1) *Affine Map:* The affine map of ellipsotopes follows from the definition. Let $E = \mathcal{E}_p(c, G, \mathcal{J}, A, b)$ with $c \in \mathbb{R}^n$ and $G \in \mathbb{R}^{n \times m}$. Consider an affine map parameterized by a matrix $T \in \mathbb{R}^{n \times n}$ and a translation vector $t \in \mathbb{R}^n$. Then

$$TE + t = \mathcal{E}_p(Tc + t, TG, A, b, \mathcal{J}). \quad (7)$$

2) *Minkowski Sum:* For the ellipsotope Minkowski sum, we use index sets to apply the p -norm separately to the coefficients from each ellipsotope, and matrix concatenation to preserve the linear constraints from the input ellipsotopes:

Proposition 3 (Minkowski Sum). Consider the ellipsotopes $E_1 = \mathcal{E}_p(c_1, G_1, A_1, b_1, \mathcal{J}_1)$ and $E_2 = \mathcal{E}_p(c_2, G_2, A_2, b_2, \mathcal{J}_2)$. Then $E_1 \oplus E_2 = E_\oplus$ for which

$$E_\oplus = \mathcal{E}_p(c_1 + c_2, [G_1, G_2], A_\oplus, b_\oplus, \mathcal{J}_\oplus), \text{ with} \quad (8a)$$

$$A_\oplus = \text{diag}(A_1, A_2), \quad b_\oplus = \begin{bmatrix} b_1 \\ b_2 \end{bmatrix}, \text{ and} \quad (8b)$$

$$\mathcal{J}_\oplus = \mathcal{J}_1 \cup (\mathcal{J}_2 + m_1), \quad (8c)$$

where m_1 is the number of generators of E_1 and $(\mathcal{J}_2 + m_1)$ is as defined in Sec. III-A.1.

Proof. By applying the definitions of Minkowski sums and ellipsotopes, we have

$$E_1 \oplus E_2 = \{x_1 + x_2 \mid x_1 \in E_1, x_2 \in E_2\} \quad (9a)$$

$$= \{c_1 + G_1\beta_1 + c_2 + G_2\beta_2 \mid \|\beta_1\langle J \rangle\|_p \leq 1 \quad (9b)$$

$$\forall J \in \mathcal{J}_1, A_1\beta_1 = b_1, \|\beta_2\langle J \rangle\|_p \leq 1, \quad (9c)$$

$$\forall J \in \mathcal{J}_2, \text{ and } A_2\beta_2 = b_2\}. \quad (9d)$$

Then, the proof is complete by taking $\beta = (\beta_1, \beta_2)$ and expanding (8) using Definition 2 and comparing to (9). Notice that \mathcal{J} ensures that the p -norm constraint is applied correctly to each subset of the coefficients of E_\oplus corresponding to E_1 and E_2 . \square

The Minkowski sum is illustrated in Figure 2.

3) *Cartesian Product:* The Cartesian product is useful for tasks such as combining reachable sets in lower dimensions to create a single, higher-dimensional reachable set for a complex system [25], [39]. To define this operation for ellipsotopes, let $E_1 = \mathcal{E}_p(c_1, G_1, A_1, b_1, \mathcal{J}_1) \subset \mathbb{R}^{n_1}$ and $E_2 =$

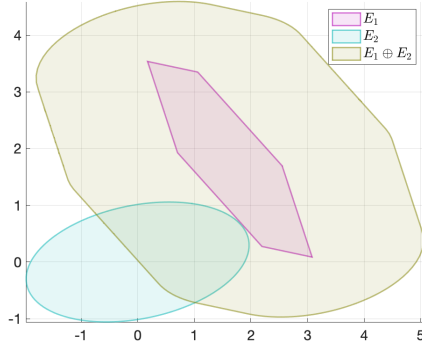


Fig. 2: Example Minkowski sum using Proposition 3.

$\mathcal{E}_p(c_2, G_2, A_2, b_2, \mathcal{J}_2) \subset \mathbb{R}^{n_2}$. By applying similar logic to the proof of Proposition 3, one can check that

$$E_1 \times E_2 = \mathcal{E}_p(c_\times, G_\times, A_\times, b_\times, \mathcal{J}_\times) \subset \mathbb{R}^{(n_1+n_2)}, \text{ with} \quad (10a)$$

$$c_\times = \begin{bmatrix} c_1 \\ c_2 \end{bmatrix}, \quad G_\times = \text{diag}(G_1, G_2), \quad (10b)$$

$$A_\times = \text{diag}(A_1, A_2), \quad b_\times = \begin{bmatrix} b_1 \\ b_2 \end{bmatrix}, \text{ and} \quad (10c)$$

$$\mathcal{J}_\times = \mathcal{J}_1 \cup (\mathcal{J}_2 + m_1), \quad (10d)$$

where m_1 is the number of generators of E_1 .

4) *Intersections*: By extending the constrained zonotope intersection property in [6], we define the intersection of ellipsotopes. Note, we do not assume this intersection is nonempty, which one can check using Proposition 7 below.

Proposition 4 (Ellipsotope Intersection). *Suppose that $E_1 = \mathcal{E}_2(c_1, G_1, A_1, b_1, \mathcal{J}_1) \subset \mathbb{R}^n$ with m_1 generators and $A_1 \in \mathbb{R}^{k_1 \times m_1}$, and $E_2 = \mathcal{E}_2(c_2, G_2, A_2, b_2, \mathcal{J}_2) \subset \mathbb{R}^n$ with m_2 generators and $A_2 \in \mathbb{R}^{k_2 \times m_2}$. Then $E_1 \cap E_2$ is an ellipsotope E_\cap given by*

$$E_\cap = \mathcal{E}_2(c_\cap, [G_\cap, 0_{n \times m_2}], A_\cap, b_\cap, \mathcal{J}_\cap), \quad (11a)$$

$$A_\cap = \begin{bmatrix} A_1 & 0_{k_1 \times m_2} \\ 0_{k_2 \times m_1} & A_2 \\ G_1 & -G_2 \end{bmatrix}, \quad b_\cap = \begin{bmatrix} b_1 \\ b_2 \\ c_2 - c_1 \end{bmatrix}, \quad \text{and} \quad (11b)$$

$$\mathcal{J}_\cap = \mathcal{J}_1 \cup (\mathcal{J}_2 + m_1). \quad (11c)$$

Proof. This follows from [6, Proposition 1] by noticing (similar to the proof of Proposition 3) that \mathcal{J} ensures that the p -norm constraints are applied separately to the coefficients of E_\cap depending on whether they came from E_1 or from E_2 . \square

This property is illustrated in Figure 3. Note that, since $E_1 \cap E_2 = E_2 \cap E_1$, one can choose which center to keep in (11a) to minimize the number of zero generators (that is, one can either add m_1 or m_2 generators). For more details on how intersections are related to the Minkowski sum, see [13].

Often, for hybrid system reachability analysis, it is necessary to detect when a reachable set intersects a hyperplane or halfspace [12], [18]. We now present both of these

intersections for ellipsotopes. As before, we do not assume in either case that the intersection is nonempty.

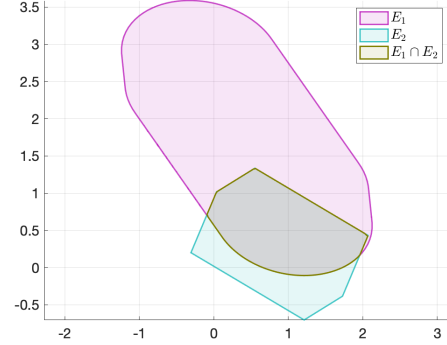


Fig. 3: Example intersection using Proposition 4.

Proposition 5 (Ellipsotope-Hyperplane Intersection). *Let $E = \mathcal{E}_p(c, G, A, b, \mathcal{J}) \subset \mathbb{R}^n$ with $c \in \mathbb{R}^n$, $G \in \mathbb{R}^{n \times m}$, $A \in \mathbb{R}^{k \times m}$, $b \in \mathbb{R}^k$, and \mathcal{J} a valid index set. Let $P = \mathcal{P}(H, f) \subset \mathbb{R}^n$ be an affine hyperplane. Then $E \cap P = E_P$ where*

$$E_P = \mathcal{E}_p(c, G, A_P, b_P, \mathcal{J}), \text{ with} \quad (12)$$

$$A_P = \begin{bmatrix} A \\ HG \end{bmatrix} \quad \text{and} \quad b_P = \begin{bmatrix} b \\ f - Hc \end{bmatrix}. \quad (13)$$

Proof. Recall that $P = \{x \in \mathbb{R}^n \mid Hx = f\}$. Then, if $x \in E \cap P$, there exists $\beta \in \mathbb{R}^m$ feasible for E , for which

$$H(c + G\beta) = f \implies HG\beta = f - Hc, \quad (14)$$

which is the last block row of the linear constraint in E_P . \square

To intersect an ellipsotope with a halfspace, we adapt [18, Theorem 1].

Proposition 6 (Ellipsotope-Halfspace Intersection). *Let $E = \mathcal{E}_p(c, G, A, b, \mathcal{J}) \subset \mathbb{R}^n$ with $c \in \mathbb{R}^n$, $G \in \mathbb{R}^{n \times m}$, $A \in \mathbb{R}^{k \times m}$, $b \in \mathbb{R}^k$, and \mathcal{J} a valid index set. Let $S = \mathcal{H}(h, s) \subset \mathbb{R}^n$, where $h \in \mathbb{R}^n$ and $s \in \mathbb{R}$. Then $E_S = E \cap S$ is given by*

$$E_S = \mathcal{E}_p(c, [G, 0_{n \times 1}], A_S, b_S, \mathcal{J}_S), \quad (15a)$$

$$A_S = \begin{bmatrix} A & 0_{k \times 1} \\ h^\top G & d \end{bmatrix}, \quad b_S = \begin{bmatrix} b \\ s - h^\top c - d \end{bmatrix} \quad (15b)$$

$$d = \frac{1}{2}(s - h^\top c + h^\top |G| 1_{m \times 1}), \quad \text{and} \quad (15c)$$

$$\mathcal{J}_S = \mathcal{J} \cup \{m+1\}, \quad (15d)$$

where $|G| \in \mathbb{R}^{n \times m}$ denotes the element-wise absolute value of the generator matrix G .

Proof. We prove this property constructively. Recall that $S = \{x \in \mathbb{R}^n \mid h^\top x \leq s\}$. Following the logic of Proposition 5, our strategy is to add a linear constraint to the coefficients β of E constraining the resulting set to lie within the halfspace; that is, we want $h^\top(c + G\beta) \leq s$. However, we need a slack variable to enforce this as an equality constraint: $h^\top(c + G\beta) + \gamma = s$, with $\gamma \geq 0$. We cannot add γ directly as a coefficient to the ellipsotope, because it is unconstrained; instead, we want to bound γ to lie within an interval, which

we can map to the interval $[-1, 1]$ containing a (scalar) ellipsotope coefficient. To do this, we first find an upper bound for γ using the fact that E is compact and lies fully within a zonotope: $E \subset \mathcal{Z}(c, G)$. From [12, Sec. 5.1], we have

$$\gamma \leq s - h^\top c + h^\top |G| \mathbf{1}_{m \times 1} \quad (16)$$

Now, we want to pick d such that, for any γ , $d(\beta_s + 1) = \gamma$ and $\|\beta_s\|_p \leq 1$, where β_s is our additional coefficient. That is, we want to find an affine transform of the interval $[-1, 1]$ to the interval $[0, s - h^\top c + h^\top |G| \mathbf{1}_{m \times 1}]$. Applying interval arithmetic, we can solve for d :

$$d([-1, 1] + 1) = [0, s - h^\top c + h^\top |G| \mathbf{1}_{m \times 1}] \quad (17)$$

$$\implies d = \frac{1}{2}(s - h^\top c + h^\top |G| \mathbf{1}_{m \times 1}) \quad (18)$$

We can then construct the necessary linear equality constraint on β and β_s as

$$h^\top (c + G\beta) + d(\beta_s + 1) = s \quad (19)$$

$$\implies h^\top G\beta + d\beta_s = s - h^\top c - d \quad (20)$$

Notice that E_S , as in (15), is the ellipsotope E with one additional coefficient and the additional linear constraint in (20), with \mathcal{J}_S ensuring that $\beta_s \in [-1, 1]$, completing the proof. \square

To build intuition for what it means when $E \cap S$ is empty, consider the zonotope $Z = \mathcal{Z}(c, G)$. Notice that, if $Z \cap S = \emptyset$, then $E \cap S = \emptyset$. In the case of the zonotope, we can interpret this to mean that the affine subspace $\mathcal{P}(A_S, b_S) \subset \mathbb{R}^{(m+1)}$ does not intersect the ∞ -norm unit ball in $\mathbb{R}^{(m+1)}$. Similarly for the ellipsotope case, the affine subspace does not intersect the ball product $\mathcal{B}_\times(\mathcal{J}_S) \subset \mathbb{R}^{(m+1)}$.

C. Emptiness and Point Containment

Given a system's state, it is often useful to check if it lies within a specific region of state space. Similarly, given a reachable set in state space, one may need to check if this set intersects with, e.g., an unsafe set. Assuming ellipsotope representation of the states and sets in question, we perform the desired checks as follows, by leveraging Proposition 4 wherein the intersection of ellipsotopes is again an ellipsotope.

Proposition 7 (Emptiness and Point Containment). *Consider the ellipsotope $E = \mathcal{E}_p(c, G, A, b, \mathcal{J}) \subset \mathbb{R}^n$ with m generators. Assume $\mathcal{P}(A, b) \neq \emptyset$. Let $x \in \mathbb{R}^n$, and let*

$$\text{cost}(\beta) = \max_{\mathcal{J} \in \mathcal{J}} \|\beta \langle \mathcal{J} \rangle\|_p, \quad (21)$$

where β is the ellipsotope coefficient vector. Then

$$E \neq \emptyset \iff \min_{\beta \in \mathbb{R}^m} \{\text{cost}(\beta) \mid A\beta = b\} \leq 1 \text{ and} \quad (22)$$

$$x \in E \iff \min_{\beta \in \mathbb{R}^m} \left\{ \text{cost}(\beta) \mid \begin{bmatrix} A \\ G \end{bmatrix} \beta = \begin{bmatrix} b \\ x - c \end{bmatrix} \right\} \leq 1, \quad (23)$$

which are both convex programs.

Proof. We prove the claim for (22), as the claim for (23) then follows from Proposition 4 by checking the emptiness

of $E \cap \mathcal{E}_p(x, [\cdot])$. Notice that, if $\beta \in \mathbb{R}^m$ is feasible for the ellipsotope definition constraints in (2), then $\text{cost}(\beta) \leq 1$ by construction. Therefore, (22) evaluates whether or not the set $\mathcal{P}(A, b)$ intersects $\mathcal{B}_\times(\mathcal{J})$ (i.e., the set of feasible β as in (6)). The constraint set is nonempty by assumption and convex by inspection. Since $\|\cdot\|_p$ is convex, and the max of convex functions is also convex, $\text{cost}(\cdot)$ is convex. \square

We find in practice that, when an ellipsotope is nonempty, it takes on the order of 10^{-5} s to solve (22), but it takes two to four orders of magnitude longer for empty ellipsotopes. However, by instead searching for a feasible β to the constraints $A\beta = b$ and $\beta \in \mathcal{B}_\times(\mathcal{J})$, we achieve much lower solve times in practice. We write the search for a feasible β as follows:

Corollary 8 (to Proposition 7). *Let $E = \mathcal{E}_p(c, G, A, b, \mathcal{J}) \subset \mathbb{R}^n$ with m generators. Assume $\mathcal{P}(A, b) \neq \emptyset$. Then*

$$E \neq \emptyset \iff \min_{\beta \in \mathbb{R}^m} \left\{ \|A\beta - b\|_2^2 \mid \beta \in \mathcal{B}_\times(\mathcal{J}) \right\} = 0. \quad (24)$$

Proof. This formulation follows directly from the fact that, for any feasible β , we have $A\beta = b$ and $\beta \in \mathcal{B}_\times(\mathcal{J})$. \square

Notice that, in the case of a constrained zonotope, (24) becomes a bounded-value least squares problem.

D. Properties of 2-Ellipsotopes

We now briefly discuss the special case of 2-ellipsotopes (i.e., ellipsotopes with $p = 2$). First, we confirm that basic 2-ellipsotopes are ellipsoids and vice-versa. Second, we notice that constrained 2-ellipsotopes are in fact basic 2-ellipsotopes. Later, in Sec. V, we leverage these properties to create an order reduction strategy for 2-ellipsotopes.

Lemma 9 (Ellipsoid-Ellipsotope Equivalence). *(Claim 1) Let $E = \mathcal{E}(c, Q) \subset \mathbb{R}^n$ be an ellipsoid as in (1). Then $E = \mathcal{E}_2(c, (\sqrt{Q})^{-1}) \subset \mathbb{R}^n$. (Claim 2) Suppose $E = \mathcal{E}_2(c, G) \subset \mathbb{R}^n$. Then there exists $Q \in \mathbb{R}^{n \times n}$, $Q \succ 0$, such that $E = \mathcal{E}(c, Q)$.*

Proof. (Claim 1) Note $(\sqrt{Q})^{-1} \succ 0$ exists because $Q \succ 0$. Suppose $x \in E$, so $(x - c)^\top Q(x - c) \leq 1$. We want to find G and β such that $(x - c) = G\beta$ and $\|\beta\|_2 \leq 1$. If we set $(G\beta)^\top Q(G\beta) = \beta^\top \beta$, then $G\beta = (\sqrt{Q})^{-1} \beta$.

(Claim 2) Suppose that $x \in E$, so there exists β such that $G\beta = x - c$. It follows from Proposition 7 that $\beta = G^\dagger(x - c)$, where G^\dagger is the Moore-Penrose pseudoinverse of G . Since $\|\beta\|_2^2 = \beta^\top \beta$, we have $\|\beta\|_2^2 = (x - c)^\top (G^\dagger)^\top (G^\dagger)(x - c)$. Then, by picking $Q = (G^\dagger)^\top (G^\dagger)$, the proof is complete. \square

While these claims are well-known in the literature (e.g., [6, (3)]), we write the proof to clarify Lemma 12 in Section V.

Next, we find a further equivalence between constrained and basic 2-ellipsotopes. To prove this, first, we confirm the well-known result that the (nonempty) intersection of an n -dimensional ellipsoid with an affine subspace is a lower-dimensional ellipsoid:

Lemma 10. *Let $B = \mathcal{B}_{2,m}$ (the m -dimensional 2-norm ball) and $H = \mathcal{P}(A, b)$ (an affine hyperplane) where $A \in \mathbb{R}^{n \times m}$ is full row rank with $n < m$, and $b \in \mathbb{R}^n$. Suppose $B \cap H \neq \emptyset$*

and $|B \cap H| > 1$. Then there exist $T \in \mathbb{R}^{m \times (m-n)}$ and $t \in \mathbb{R}^m$ such that $T\mathcal{B}_{2,m-n} + t = B \cap H \subset \mathbb{R}^m$.

Proof. We construct $t = A^\dagger b \in H$. Notice that $t \in H$ because $n < m$. Then, $t \in B$ because it is a least-squares solution and $B \cap H \neq \emptyset$. To construct T , let $p \in \text{bd}(B \cap H)$, so $\|p\|_2 = 1$. Since $|B \cap H| > 1$, we have $\|t\|_2 < 1$. Let $c = \|p - t\|_2$, and note $c < 1$ by the triangle inequality. Also by triangle inequality, for any $q \in B \cap H$, if $\|q - t\|_2 \neq c$, then $\|q\|_2 \neq 1$. Let $K = \{e_1, \dots, e_{m-n}\} \subset \mathbb{R}^m$ be an orthonormal basis for $\ker(A)$. Then $T = [ce_1, \dots, ce_{m-n}]$. \square

Lemma 11 (Basic and Constrained 2-Ellipsoid Equivalence). *Let $E = \mathcal{E}_2(c, G, A, b)$ be a nonempty constrained ellipsoid with $A \in \mathbb{R}^{k \times m}$, $b \in \mathbb{R}^k$, and $k < m$. Then there exist c', G' such that $E = \mathcal{E}_2(c', G')$.*

Proof. This follows from Lemma 10. Since E is nonempty, we can construct an affine map parameterized by T and t such that $T\mathcal{B}_{2,m-k} + t = B \subset \mathbb{R}^m$. Then, for any $\beta \in \mathcal{B}_{2,m-k}$, we have $c + G(T\beta + t) \in E$. Choose $c' = c + Gt$ and $G' = GT$ to complete the proof. \square

Note that 2-ellipsoids let us represent ellipsoidal Gaussian confidence level sets. We demonstrate this via a robot path verification example in Sec. VI-C.

E. Relationships to Other Set Representations

1) Ellipsoids, Zonotopes, and Similar Representations:

Per Lemma 9, ellipsoids generalize ellipsoids and, as a corollary, superellipsoids. We see from the Definition 2, specifically (5) that ellipsoids generalize (constrained) zonotopes, by comparison to (2). In particular, if the index set $\mathcal{J} = \{\{1\}, \{2\}, \dots, \{m\}\}$ for an ellipsoid with m generators, then the ellipsoid is also a (constrained) zonotope.

Another useful set representation is the *capsule*, often used to represent robot manipulator links for efficient collision detection [40], [41]. A capsule is the Minkowski sum of a line segment with a sphere, which we can represent as an ellipsoid per Lemma 9 and Proposition 3. Importantly, ellipsoids allow us to generalize capsules to Minkowski sums of line segments with, e.g., confidence level set ellipsoids of a Gaussian distribution.

2) *Constrained Polynomial Zonotopes:* We can also show that every ellipsoid is a CPZ as in (4) by applying similar logic to the proof that every ellipsoid is a CPZ [24]. Consider the basic case of $E = \mathcal{E}_p(c, G)$. Then,

$$E = \left\{ c + G\beta \mid \|\beta\|_p \leq 1 \right\} \quad (25)$$

$$= \left\{ c + [G, 0](\beta, \beta_s) \mid 0.5\beta_s + \|\beta\|_p^p = 0.5, \text{ and } \|\beta, \beta_s\|_\infty \leq 1 \right\}, \quad (26)$$

where $\beta_s \in \mathbb{R}$ acts as a slack variable. Then the ellipsoid is $E = \mathcal{CPZ}(c, G, X, A, b, D)$ with $X = I_m$, $b = 0.5 \cdot \mathbf{1}_{k \times 1}$, and $D = k \cdot \mathbf{1}_{p \times 1}$. Adding linear constraints or an index set on the coefficients of E necessitates only minor changes to A , b , and D in the CPZ formulation.

V. ORDER REDUCTION

A commonly-used operation in zonotope reachability analysis is order reduction, or the approximation of a zonotope by a new zonotope with fewer generators. This operation is necessary because reachability analysis commonly uses Minkowski sums, which increase the number of generators of a zonotope (or ellipsoid, per Proposition 3).

A variety of order reduction techniques exist for zonotopes, most commonly achieved by enclosing a subset of a zonotope's generators in a bounding box, the sides of which become new generators [11], [12]. This strategy can be improved or guided by a variety of heuristics [2, Ch. 2]. In the case of polynomial zonotopes, which are not necessarily convex, one can apply a similar strategy of overapproximating a subset of generators with a zonotope or interval [23], [25]. For constrained zonotopes, the linear constraints necessitate alternative strategies [6], [18].

To proceed, we discuss order reduction for 2-ellipsoids leveraging ellipsoid techniques. We then comment on more general strategies.

A. Order Reduction for 2-Ellipsoids

For 2-ellipsoids, we can leverage the properties of ellipsoids to perform order reduction.

1) *Basic 2-Ellipsoids:* First, we note that a basic 2-ellipsoid in \mathbb{R}^n never requires more than n generators:

Lemma 12 (Exact Order Reduction of Basic 2-Ellipsoids). *Let $E = \mathcal{E}_2(c, G) \subset \mathbb{R}^n$ with $G \in \mathbb{R}^{n \times m}$ full row rank and $m > n$. Then $E = \mathcal{E}_2(c, \tilde{G})$, where*

$$\tilde{G} = \left(\sqrt{(G^\dagger)^\top (G^\dagger)} \right)^{-1}. \quad (27)$$

and G^\dagger is the Moore-Penrose pseudoinverse of G .

Proof. This follows from Lemma 9, by converting E to an ellipsoid, then back to an ellipsoid. Note, the matrix in the outermost parentheses of (27) is invertible because it is the square root of a positive definite matrix. \square

Notice that $\tilde{G} \in \mathbb{R}^{n \times n}$, so E needs only n generators.

2) *General Strategy for 2-Ellipsoids:* Our general strategy is to treat 2-ellipsoids as a Minkowski sum of ellipsoids. This is because order reduction is usually necessary after several Minkowski sum operations result in a large number of generators during, e.g., reachability analysis.

To explain our approach, we consider a simple case. Consider $E = \mathcal{E}_2(c, G, A, b, \mathcal{J}) \subset \mathbb{R}^n$ with $m > n$ generators and with k linear constraints. Suppose that we can write $E = E_1 \oplus E_2$ where $E_1 = \mathcal{E}_2(c_1, G_1, A_1, b_1)$ with m_1 generators and $E_2 = \mathcal{E}_2(c_2, G_2, A_2, b_2)$ with m_2 generators. Notice that $m = m_1 + m_2$. Our goal is to find \tilde{E} for which $\tilde{E} = \mathcal{E}_2(c', G') \supseteq E$.

First, by Lemma 11, we can find t_1 and T_1 such that $E_1 = \mathcal{E}_2(c_1 + G_1 t_1, G_1 T_1)$, and similarly for E_2 . Then, per Lemma 9, we can find Q_1 to represent E_1 as an ellipsoid, $E_1 = \mathcal{E}(c_1 + G_1 t_1, Q_1)$, and similarly we can find Q_2 for E_2 .

We now apply the method in [14] to create a minimum-volume outer ellipsoid (MVOE) $E_{\text{rdc}} \supseteq E_1 \oplus E_2$. That is, we

can write $E_{\text{rdc}} = \mathcal{E}(c_{\text{rdc}}, Q_{\text{rdc}}) \supset E_1 \oplus E_2$. By Lemma 9, we know that $E_{\text{rdc}} \supset E$. By Lemma 12, we know that E_{rdc} needs no more than $n < m$ generators. Therefore, we can choose $\tilde{E} = E_{\text{rdc}}$.

3) *Choosing Which Ellipsoids to Overapproximate:* The above example considered an ellipsoid created as the Minkowski sum of a pair of ellipsoids, so the order reduction strategy was to overapproximate this sum with a single ellipsoid. We now extend this idea to the case when an ellipsoid is a Minkowski sum of many ellipsoids.

First, we set up our assumptions. Consider again the ellipsoid $E = \mathcal{E}_2(c, G, A, b, \mathcal{J}) \subset \mathbb{R}^n$ with m generators. Assume that we can write E as the Minkowski sum of several basic 2-ellipsotopes, which we call *component ellipsotopes*:

$$E = E_1 \oplus E_2 \oplus \cdots \oplus E_r, \quad (28)$$

for some $r \in \mathbb{N}$. That is, each $E_i = \mathcal{E}_2(c_i, G_i)$. Notice that E requires at most $r \times n$ generators.

Now, suppose that we want to find \tilde{E} such that $\tilde{E} \supset E$ and \tilde{E} has $m - n$ generators; in other words, we want to reduce the number of 2-ellipsotopes in (28) by one. To do so, we choose $i, j \in \mathbb{N}_r$ and construct $E_{\text{rdc}} = E_i \oplus E_j$ such that

$$\tilde{E} = \left(\bigoplus_{l \in \mathbb{N}_r \setminus \{i, j\}} E_l \right) \oplus E_{\text{rdc}}. \quad (29)$$

The question is then how to choose i and j . Our goal for choosing i and j is to minimize the conservatism introduced by overapproximating $E_i \oplus E_j$.

The most straightforward option is to choose the (i, j) pair for which the MVOE has the smallest volume. We do this by applying the standard formula for the volume of an n -dimensional hyperellipsoid; if $E = \mathcal{E}(c, Q) \subset \mathbb{R}^n$, then $\text{volume}(E) = \det((\sqrt{Q})^{-1}) \frac{2}{n} \frac{\pi^{n/2}}{\Gamma(n/2)}$, where $\det(\cdot)$ denotes the determinant and Γ is the well-known gamma function. Since $G = (\sqrt{Q})^{-1}$ is the generator matrix given by Lem. 9 and all component ellipsotopes share the same dimension n , we can choose those for which $\det(G)$ is smallest.

However, we need an easier-to-compute heuristic when multiple ellipsoids have nearly-identical volumes or when there are many high-dimensional ellipsoids for which computing the MVOE and volume of every (i, j) pair is intractable. We find in practice that, when the longest axes of E_1 and E_2 are nearly perpendicular, the resulting MVOE is a more conservative overapproximation. Therefore, we pick i and j to find the pair of longest ellipsoid axes that are closest to parallel:

$$(i, j) = \arg \max_{i, j \in \mathbb{N}_r} \left| v_i^\top v_j \right| \quad (30)$$

where v_i (resp. v_j) is the unit vector in the direction of the longest semi-axis of E_i (resp. E_j). That is, v_i is the eigenvector of Q_i^{-1} corresponding to its largest eigenvalue.

4) *Identifying Component Ellipsotopes:* In Section IV-B, we found that intersections between ellipsotopes, hyperplanes, and halfspaces all introduce linear constraints. Strategies exist to conservatively simplify these linear constraints

for constrained zonotopes [6], [18]. For 2-ellipsotopes, we can instead use the index set and constraints to identify component ellipsotopes.

Notice that all intersections introduce a new block row to the ellipsoid constraints (see Propositions 4, 5, and 6), while placing any existing constraints either block-diagonally (in the case of ellipsoid-ellipsoid intersection) or with zero-padding (for halfspace intersection). Furthermore, the ellipsoid's index set contains the indices of the columns corresponding to the constraints that existed before the intersection procedure. Therefore, given an arbitrary ellipsoid, if we identify indices in the index set that correspond to a block-diagonal arrangement of linear constraints, then we can extract the component ellipsotopes and simplify them with Lemma 11.

To illustrate this idea with an example, consider an ellipsoid $E = \mathcal{E}_2(c, G, A, b, \mathcal{J})$ with m generators. Suppose that $A = \text{diag}(A_1, A_2) \in \mathbb{R}^{2 \times m}$, $A_1 \in \mathbb{R}^{1 \times m_1}$, and $A_2 \in \mathbb{R}^{1 \times m_2}$. Also suppose $\mathcal{J} = \{\mathbb{N}_{m_1}, \mathbb{N}_{m_2} + m_1\}$. Then

$$E = \mathcal{E}_2(c, G(\cdot, \mathbb{N}_{m_1}), A_1, b(\mathbb{N}_{m_1})) \oplus \mathcal{E}_2(c, G(\cdot, \mathbb{N}_{m_2}), A_2, b(\mathbb{N}_{m_2})). \quad (31)$$

In other words, we have broken E into two component ellipsotopes, which we can then reduce as above.

B. General Strategies for Order Reduction

We now briefly discuss order reduction when $p \neq 2$. In short, strategies from the literature for zonotopes and constrained zonotopes still apply to ellipsotopes. We leave strategies that leverage the p -norm structure to future work.

1) *Leveraging Component Zonotopes:* We noted above that order reduction for an arbitrary 2-ellipsoid follows from treating it as a Minkowski sum of component ellipsoids. For a basic p -ellipsoid, we can adopt a similar strategy by considering component zonotopes.

First, notice that, by making a single generator's p -norm constraint independent from all other generators, we overapproximate an ellipsoid. We call this *popping* a generator:

Lemma 13 (Generator Popping). *Consider the indexed ellipsoid $E = \mathcal{E}_p(c, G, \mathcal{J})$. Consider an arbitrary $J \in \mathcal{J}$ and suppose $j \in J$. Define $\tilde{J} = (J \setminus \{j\})$ and $\tilde{\mathcal{J}} = (\mathcal{J} \setminus J) \cup \tilde{J} \cup \{j\}$. Then $E \subset \tilde{E}$ where $\tilde{E} = \mathcal{E}_p(c, G, \tilde{\mathcal{J}})$.*

Proof. For any feasible β , $\|\beta\langle J \rangle\|_p \leq \|\beta\langle \tilde{J} \rangle\|_p + |\beta\langle j \rangle|$ by the triangle inequality. \square

Then, a strategy for order reduction is as follows. Suppose $E \subset \mathbb{R}^n$ has m generators, and we seek to remove n_{rdc} of them. First, we pop the $n_{\text{rdc}} + n$ smallest (in the 2-norm) generators. Let $G = [G_{\text{keep}}, G_{\text{rdc}}]$ where G_{rdc} contains these $n_{\text{rdc}} + n$ generators; note we can reorder G in this way without loss of generality. Let $Z_{\text{rdc}} = \mathcal{E}_p(0, G_{\text{rdc}}, \{\{1\}, \{2\}, \dots, \{n_{\text{rdc}}\}\})$, which is a zonotope by construction. If we pop the G_{rdc} generators, then $E = \mathcal{E}_p(c, G_{\text{keep}}, \mathcal{J}_{\text{keep}}) \oplus Z_{\text{rdc}}$, where $\mathcal{J}_{\text{keep}}$ is the original index set with the indices corresponding to G_{rdc} removed, and then reorganized to match G_{keep} . Finally, we can apply zonotope order reduction (e.g., from [2], [11],

[12]) to find an n -dimensional interval $\tilde{Z}_{\text{rdc}} \supseteq Z_{\text{rdc}}$, which can be represented as an ellipsotope with n generators (each with the p -norm constraint applied separately).

We briefly note that generator popping enables further simplification in the $p = 2$ case, wherein one can overapproximate the zonotope created by all popped generators by a single ellipsoid using the technique in [38].

2) *Constraint Reduction*: For $p \neq 2$, the result in Lemma 11 no longer holds; that is, the intersection of a superellipsoid with an affine subspace is not always an affine map of a lower-dimensional superellipsoid, which can be seen by considering the ∞ -norm ball intersecting a plane. However, the constraint reduction strategies from [6] and [18] still apply. In particular, we can eliminate a constraint by adapting [6, Proposition 5]:

Proposition 14. *Let $E = \mathcal{E}_p(c, G, A, b, \mathcal{J}) \subset \mathbb{R}^n$ with m generators and k constraints. Let $\Gamma \in \mathbb{R}^{n \times k}$ and $\Lambda \in \mathbb{R}^{k \times k}$. Then*

$$E \subseteq \tilde{E} = \mathcal{E}_p(c + \Gamma b, G - \Gamma A, A - \Lambda A, b - \Lambda b, \mathcal{J}). \quad (32)$$

Proof. Let $x \in E$, so there exists $\beta \in \mathbb{R}^m$ such that $x = c + G\beta$ and $A\beta = b$. It then follows that $x = c + G\beta + \Gamma(b - A\beta)$ and $A\beta = b + \Lambda(b - A\beta)$. \square

By choosing Λ as a matrix of zeros with a single one on the diagonal, one can cause a row of $[A, b]$ to become zeros, thereby eliminating a constraint and producing an overapproximation. Note that [6] presents a further strategy for eliminating a constraint and a generator by choosing both Γ and Λ . We leave adapting this strategy to future work.

VI. EXAMPLES

We now demonstrate properties and uses of ellipsotopes; in particular, we illustrate fault detection, assess the speed of the emptiness check, verify collision-avoidance for robot path planning under uncertainty, and show order reduction. All examples are run on a desktop computer with a 6-core 3.6 GHz processor and 32 GB of RAM¹.

A. Fault Detection

We implement the set-based fault detection example from [6, Section 6], in which a nominal model is given and a faulty model is propagated. A set-based estimator is propagated using the nominal dynamics and a set-inclusion check is performed at each timestep. The goal is to detect the fault, i.e. discrepancy between the nominal and faulty model, in the least number of timesteps. Using ellipsotopes, we are able to detect the fault in average of 23.54 timesteps over 500 simulation runs, compared to 27.718 when using constrained zonotopes as demonstrated in [6]. By maintaining tighter set representations, ellipsotopes lead to fewer missed detections and lower time to detect. In addition, ellipsotopes allow for fault detection with ellipsoid-like sets. Running the same example while using ellipsoids results in the fault being failed to be detected, due to the overapproximation of ellipsoid intersection.

¹All code used for figures and examples is available online at <https://github.com/Stanford-NavLab/ellipsotopes>.

B. Emptiness Checking

We now evaluate how long it takes to check if an ellipsotope is empty using Cor. 8. We apply Cor. 8 because we find in practice that solving the feasibility problem (24) is orders of magnitude faster than solving (22) from Prop. 7. This speed-up is because there is often a continuum of optimal solutions to (24), but only one optimal solution to (22).

Our evaluation method is as follows. First, we generate 10 random 2-D 2-ellipsotopes for each $m = 1, 2, \dots, 20$ generators (each generator of length no more than $1/m$) and $k = 1$ linear constraint. Then, we set $b = 0_{k \times 1}$ or $b = 2m \cdot 1_{k \times 1}$ (which ensures emptiness). Finally, we solve (24) using MATLAB's `fmincon` solver with an initial guess of $\beta_0 = A^\dagger b$, and compute the solve time with MATLAB's `timeit` tool.

The results, summarized in Fig. 4, show that it takes on the order of 10^{-5} s to confirm that an ellipsotope is nonempty, whereas it takes on the order of 10^{-2} s to identify that an ellipsotope is empty. This is because, for a nonempty ellipsotope, the initial guess of $A^\dagger b$ is often a feasible solution to (24), so the solver can terminate on the first iteration. In either case, this experiment demonstrates that ellipsotopes enable fast emptiness checking on the order of 10^{-2} s with a naïve MATLAB implementation.

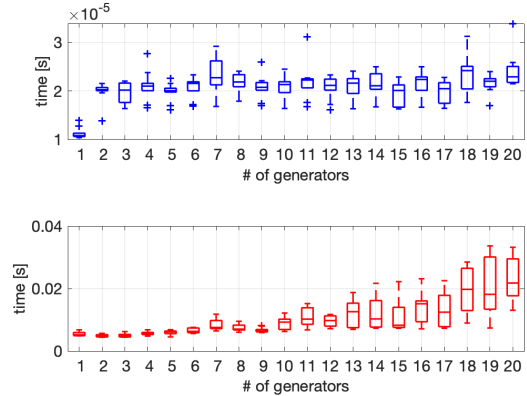


Fig. 4: Timing results for solving the ellipsotope emptiness check (24) as a function of the number of generators for random 2-dimensional 2-ellipsotope. The top (resp. bottom) subplot shows the emptiness check times for nonempty (resp. empty) ellipsotopes. The box-and-whisker plots represent the 25-75% interquartile range (box), median (line through box), min/max of data (whiskers), and outliers (plus signs). Empty ellipsotopes typically take more time because they require multiple iterations to solve (24) instead of terminating early upon finding a single feasible solution.

C. Robot Path Verification

We now present a planar path verification example in which ellipsotopes are used to represent the reachable set of the combined volume of a robot's body and its uncertainty in state. This example illustrates the practicality of the ellipsotope Minkowski sum, intersection, and emptiness check

properties. To demonstrate that ellipsotopes can provide tighter bounding reachable sets than zonotopes or ellipsoids, we also compute the reachable sets for the same trajectory using both zonotopes and ellipsoids using the CORA toolbox [42].

1) *System Dynamics and Measurements:* We consider a robot with a box-shaped rigid body with width w_{rob} and length l_{rob} , and represent it with the 2-ellipsotope:

$$E_{\text{rob}} = \mathcal{E}_2 \left(0_{2 \times 1}, \frac{1}{2} \text{diag}(w_{\text{rob}}, l_{\text{rob}}), \{\{1\}, \{2\}\} \right), \quad (33)$$

We model the system with discrete-time, nonlinear dynamics and measurements. In particular we consider a Dubins car model with state $x(t) = [x_1(t), x_2(t), \theta(t)]^\top$, input $u(t) = [v(t), \omega(t)]^\top$ and center-of-mass equations of motion

$$x_1(t) = x_1(t-1) + v(t-1) \cos(\theta(t-1)) \Delta_t + w_1(t) \quad (34a)$$

$$x_2(t) = x_2(t-1) + v(t-1) \sin(\theta(t-1)) \Delta_t + w_2(t) \quad (34b)$$

$$\theta(t) = \theta(t-1) + \omega(t-1) \Delta_t + w_3(t), \quad (34c)$$

where $p(t) = [x_1(t), x_2(t)]^\top$ is the robot's center-of-mass position and $\theta(t)$ is its heading at time $t \in \mathbb{N}$. The process noise is $w(t) \sim \mathcal{N}(0, Q)$ where $Q \in \mathbb{R}^{3 \times 3}$ and $Q \succ 0$. The control inputs are longitudinal speed $v(t)$ and yaw rate $\omega(t)$. Time is discretized by $\Delta_t = 0.1$ s.

The robot's measurements consist of 4 ranges to beacons placed at fixed, known locations, as well as a heading measurement, all with additive Gaussian noise. Range measurements that are taken when $x_1(t) < 30$ have noise variance of 0.4 m, while measurements taken when $x_1(t) \geq 30$ (shown shaded in light red in Fig. 6) have a higher variance of 10.0 m.

2) *Reachability under Position Uncertainty:* The robot tracks a nominal trajectory $(\check{x}(1), \dots, \check{x}(N))$ with a linear state estimator and controller, as in [43] and [3]. At time t the state estimator provides an uncertain estimate of the robot's state parameterized by the mean and covariance of the Gaussian distribution $\mathcal{N}(\mu(t), \Sigma(t))$. We assume the position and heading covariance are decoupled, such that we can decompose $\mu(t)$ and $\Sigma(t)$ into position and heading components:

$$\mu(t) = \begin{bmatrix} \mu_p(t) \\ \mu_\theta(t) \end{bmatrix}, \quad \Sigma(t) = \text{diag}(\Sigma_p(t), \Sigma_\theta(t)). \quad (35)$$

Now consider the α -probability confidence level set of the robot's uncertain position, E_{unc} , for which $P(p(t) \in E_{\text{unc}}) \geq \alpha$. We can express E_{unc} as the ellipse

$$E_{\text{unc}} = \{x + \check{p}(t) \mid x^\top (\varepsilon \Sigma_p(t))^{-1} x \leq 1\}, \quad (36)$$

$$\varepsilon = -2 \log(1 - \alpha). \quad (37)$$

Using Lemma 9, we represent this ellipse with the 2-ellipsotope: $E_{\text{unc}}(t) = \mathcal{E}_2(\check{p}(t), (\varepsilon \Sigma_p(t))^{1/2})$. Given some initial state estimation covariance Σ_0 , we propagate state uncertainty along the nominal trajectory according to [43, Equations (17)-(21) and (33)], and obtain the associated α -confidence ellipses that enclose the center-of-mass trajectory of the robot, under uncertainty due to noisy dynamics and measurements, with probability α .

3) *Handling Robot Body and Heading Uncertainty:* To account for the robot's body, we cannot simply Minkowski sum the E_{rob} ellipsotope with the E_{unc} ellipsotope, because we must account for heading uncertainty. We do so by first taking the α -confidence interval, $(\check{\theta} - \Delta_\theta, \check{\theta} + \Delta_\theta)$, of the distribution $\mathcal{N}(\check{\theta}, \Sigma_\theta)$ of heading (θ) estimates. Next, to overbound the area swept out by the robot's body over this range of angles, we create an ellipsotope as the intersection of the circumscribing circle of the robot's body with four halfplanes, shown in Figure 5. Then, for each timestep of the trajectory, we Minkowski sum this ellipsotope with the center of mass confidence ellipse from position uncertainty propagation to obtain a reachable set that accounts for the robot's body plus position and heading uncertainty.

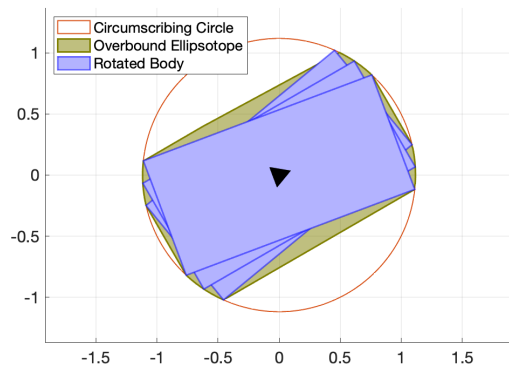


Fig. 5: Construction of an ellipsotope (dark yellow) which encloses a rectangular robot body (as in Sec. VI-C) under a confidence interval of uncertain headings (two different possible rotations of the body shown in blue, with the heading as a black arrow).

4) *Collision Checking and Area Approximation:* For each of the 187 timesteps of the nominal trajectory, we compute the intersection between the reachable set and each obstacle. We then solve the emptiness check in Cor. 8 to assess if the reachable set is in collision. To collision check the comparison ellipsoid and zonotope reachable sets, we overapproximate the obstacles as ellipsoids and zonotopes respectively, allowing us to use the CORA intersection and emptiness check implementations for comparison.

We compute the total area of each 2-D reachable set to assess conservatism. For ellipsotopes, we approximate area by sampling points from the boundary, constructing a polygon from the sampled points, then computing the area of the polygon. For zonotopes and ellipsoids we use the CORA built-in functions for computing area.

5) *Results and Discussion:* The ellipsotope reachable set is computed in 52.13 ms and collision checked in 8.14 s. Given that 187 timesteps is a 18.7 s long trajectory, this shows that we can validate uncertain trajectories with ellipsotope reachable sets faster than real time. For comparison, we also time the collision check of the zonotope and ellipsoid reachable sets with the obstacles. The zonotope reachable set is collision checked in 3.16 s and the ellipsoid reachable set in 0.25 s. Thus, ellipsotopes require slightly

more computation but provide a more accurate reachable set representation.

For the sake of comparison, the ellipsoid, zonotope, and ellipsotope reachable sets are shown together in Figure 6. The zonotope reachable set has an area of 2893.26 m², the ellipsoids 2399.94 m², and the ellipsotopes 2274.73 m². Thus, ellipsotopes provide a tighter reachable set than zonotopes or ellipsoids, as we would expect.

This example illustrates how ellipsotopes can tightly represent reachable sets of systems with uncertainty and geometric shape. Furthermore, we can use intersections and emptiness checking (Properties 4 and 7) to efficiently perform collision checking of this reachable set with obstacles also represented by ellipsotopes. Also note, this example is an improvement over [3], since we *exactly represent* the confidence bounds of the uncertain position and heading states as ellipsotopes, instead of overapproximating the bounds with zonotopes.

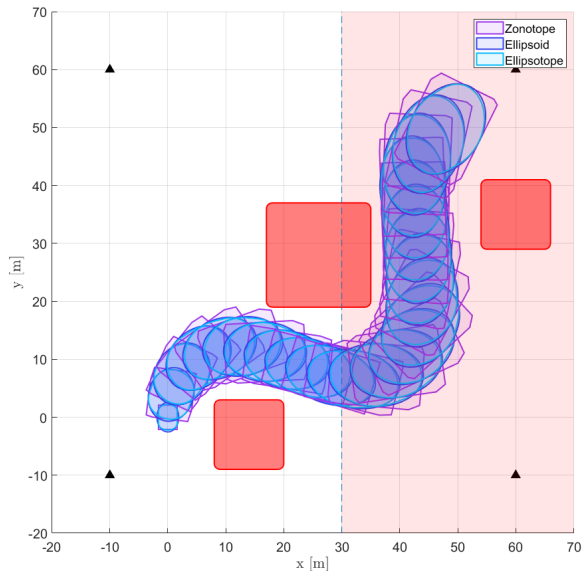


Fig. 6: Comparison of reachable sets represented by zonotopes, ellipsoids, and ellipsotopes, each shown with a different color. Although the ellipsoid and ellipsotope reachable sets, the ellipsotopes are able to more tightly bound the robot’s body, thus resulting in an overall tighter reachable set.

D. Order Reduction

We provide two brief examples of order reduction.

1) *Method for 2-Ellipsotopes:* We demonstrate the order-reduction heuristic in (30) on an example with three 2-ellipsotopes. First, we create $E_1 = \mathcal{E}_2(0_{2 \times 1}, G_2)$ with

$$G_1 = \begin{bmatrix} 3 & 2 \\ -1 & 0 \end{bmatrix}. \quad (38)$$

Then, we create E_2 by rotating G_1 by $\pi/6$ radians and E_3 by rotating G_1 by $\pi/2$ radians, as shown in Fig. 7.

Next, we consider the possible (i, j) pairs of ellipsotopes to overapproximate with an MVOE. The heuristic values for the different pairs are shown in Tab. I. We maximize the

heuristic by picking $(i, j) = (1, 2)$ (i.e., finding the MVOE of $E_1 \oplus E_2$).

We assess the heuristic as follows. First, for each possible (i, j) combination, we compute the ratio between the area of the reduced ellipsotope and the area of the exact Minkowski sum $E = E_1 \oplus E_2 \oplus E_3$. We approximate each ellipsotope’s area using the method discussed above in the path planning example. We similarly approximate the Hausdorff distance between each reduced ellipsotope and the exact Minkowski sum ellipsotope. For both the area ratio and Hausdorff distance, our heuristic’s chosen pair (1,2) is the lowest, meaning our outer-approximation is the least conservative. The results are summarized in Tab. I, and the Minkowski sums of the different (i, j) pairs are shown in Fig. 7.

(i, j)	Heuristic	Area Ratio	Hausdorff Dist.	MVOE Area
(1,2)	0.87	1.05	0.40	49.07
(1,3)	0.00	1.05	0.42	87.96
(2,3)	0.50	1.16	1.05	77.28

TABLE I: Order reduction heuristic results; we see that the heuristic from (30) for reducing 2-ellipsotopes produces the tightest overapproximation by replacing a Minkowski sum of ellipsoids with a single ellipsoid. The (i, j) pairs index which of the three ellipsotopes in the left subplot of Fig. 7 are being Minkowski summed.

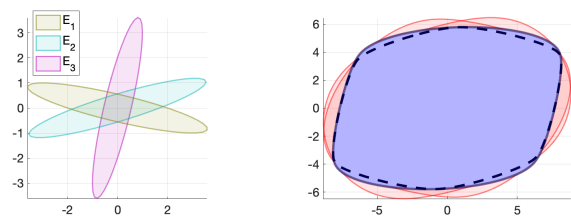


Fig. 7: Example of order reduction heuristic (30) for an ellipsotope constructed as the Minkowski sum of three 2-ellipsotopes (left subplot). The right subplot shows the exact Minkowski sum as a dashed line, the reduced ellipsotope chosen by the heuristic in light blue, and the other two possible reduced ellipsotopes in red. The heuristic result is the closest overapproximation to the exact result by the metrics in Tab. I.

2) *General Method:* We apply the technique from [6, Proposition 5] to eliminate a single constraint. We create a random 2-D 2-ellipsotope with 8 generators and 2 constraints. We remove each constraint separately to produce two different overapproximations as shown in Figure 8.

VII. CONCLUSION

This work introduced ellipsotopes, a novel set representation created by generalizing the ∞ -norm that defines zonotopes and constrained zonotopes. We illustrated that this set representation is closed under the operations critical to reachability analysis and fault detection: affine transformations, Minkowski sum, and intersection. Since ellipsotopes can grow in complexity similar to zonotopes when used for

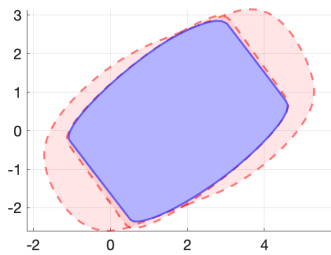


Fig. 8: Constraint reduction of the blue ellipsotope, which has two constraints. Each red dashed outlined ellipsotope results from eliminating one constraint.

reachability analysis, we discussed several order reduction strategies. We also demonstrated the various properties of ellipsotopes via numerical examples, and illustrated their importance via a literature comparison to other set representations. For future work, we intend to formalize a stochastic variant of ellipsotopes and discover more applications of these objects to tasks in reachability, fault detection, and navigation. We also intend to explore applications of ellipsotopes in neural network verification.

REFERENCES

[1] S. Kousik, S. Vaskov, F. Bu, M. Johnson-Roberson, and R. Vasudevan, "Bridging the gap between safety and real-time performance in receding-horizon trajectory design for mobile robots," *The International Journal of Robotics Research*, vol. 39, no. 12, pp. 1419–1469, 2020.

[2] M. Althoff, "Reachability analysis and its application to the safety assessment of autonomous cars," Ph.D. dissertation, Technische Universität München, 2010.

[3] A. Shetty and G. X. Gao, "Predicting State Uncertainty Bounds Using Non-Linear Stochastic Reachability Analysis for Urban GNSS-Based UAS Navigation," *IEEE Transactions on Intelligent Transportation Systems*, 2020.

[4] M. Chen, S. Herbert, H. Hu, Y. Pu, J. F. Fisac, S. Bansal, S. Han, and C. J. Tomlin, "Fastrack: a modular framework for real-time motion planning and guaranteed safe tracking," *IEEE Transactions on Automatic Control*, 2021.

[5] S. Bhamidipati and G. X. Gao, "Integrity-Driven Landmark Attention for GPS-Vision Navigation via Stochastic Reachability," in *Proceedings of the 33rd International Technical Meeting of the Satellite Division of The Institute of Navigation (ION GNSS+ 2020)*, 2020, pp. 2311–2326.

[6] J. K. Scott, D. M. Raimondo, G. R. Marseglia, and R. D. Braatz, "Constrained zonotopes: A new tool for set-based estimation and fault detection," *Automatica*, vol. 69, pp. 126–136, 2016.

[7] A. D. Ames, X. Xu, J. W. Grizzle, and P. Tabuada, "Control barrier function based quadratic programs for safety critical systems," *IEEE Transactions on Automatic Control*, vol. 62, no. 8, pp. 3861–3876, 2016.

[8] N. Smit-Anseeuw, C. D. Remy, and R. Vasudevan, "Walking with confidence: Safety regulation for full order biped models," *IEEE Robotics and Automation Letters*, vol. 4, no. 4, pp. 4177–4184, 2019.

[9] A. B. Kurzanski and P. Varaiya, "Ellipsoidal techniques for reachability analysis," in *International Workshop on Hybrid Systems: Computation and Control*, Springer, 2000, pp. 202–214.

[10] A. A. Kurzanskiy and P. Varaiya, "Ellipsoidal toolbox (ET)," in *Proceedings of the 45th IEEE Conference on Decision and Control*, IEEE, 2006, pp. 1498–1503.

[11] C. Combastel, "A state bounding observer for uncertain non-linear continuous-time systems based on zonotopes," in *Proceedings of the 44th IEEE Conference on Decision and Control*, IEEE, 2005, pp. 7228–7234.

[12] A. Girard, "Reachability of uncertain linear systems using zonotopes," in *International Workshop on Hybrid Systems: Computation and Control*, Springer, 2005, pp. 291–305.

[13] L. J. Guibas, A. T. Nguyen, and L. Zhang, "Zonotopes as bounding volumes," in *SODA*, vol. 3, 2003, pp. 803–812.

[14] A. Halder, "On the parameterized computation of minimum volume outer ellipsoid of Minkowski sum of ellipsoids," in *2018 IEEE Conference on Decision and Control (CDC)*, IEEE, 2018, pp. 4040–4045.

[15] E. A. Yildirim, "On the minimum volume covering ellipsoid of ellipsoids," *SIAM Journal on Optimization*, vol. 17, no. 3, pp. 621–641, 2006.

[16] S. Sadraddini and R. Tedrake, "Linear encodings for polytope containment problems," in *2019 IEEE 58th Conference on Decision and Control (CDC)*, IEEE, 2019, pp. 4367–4372.

[17] M. Kvasnica, P. Grieder, M. Baotić, and M. Morari, "Multi-parametric toolbox (MPT)," in *International workshop on hybrid systems: Computation and control*, Springer, 2004, pp. 448–462.

[18] V. Raghuraman and J. P. Koeln, "Set operations and order reductions for constrained zonotopes," *arXiv preprint arXiv:2009.06039*, 2020.

[19] A. Girard and C. Le Guernic, "Efficient reachability analysis for linear systems using support functions," *IFAC Proceedings Volumes*, vol. 41, no. 2, pp. 8966–8971, 2008.

[20] C. Le Guernic and A. Girard, "Reachability analysis of hybrid systems using support functions," in *International Conference on Computer Aided Verification*, Springer, 2009, pp. 540–554.

[21] —, "Reachability analysis of linear systems using support functions," *Nonlinear Analysis: Hybrid Systems*, vol. 4, no. 2, pp. 250–262, 2010.

[22] M. Althoff, "Reachability analysis of nonlinear systems using conservative polynomialization and non-convex sets," in *Proceedings of the 16th international conference on Hybrid systems: computation and control*, 2013, pp. 173–182.

[23] N. Kochdumper and M. Althoff, "Sparse polynomial zonotopes: A novel set representation for reachability analysis," *IEEE Transactions on Automatic Control*, 2020.

[24] —, "Constrained polynomial zonotopes," *arXiv preprint arXiv:2005.08849*, 2020.

[25] "Reachable Sets for Safe, Real-Time Manipulator Trajectory Design," in *Proceedings of Robotics: Science and Systems*, Corvallis, Oregon, USA, Jul. 2020.

[26] P. S. Duggirala and M. Viswanathan, "Parsimonious, simulation based verification of linear systems," in *International Conference on Computer Aided Verification*, Springer, 2016, pp. 477–494.

[27] S. Bak and P. S. Duggirala, "Simulation-equivalent reachability of large linear systems with inputs," in *International Conference on Computer Aided Verification*, Springer, 2017, pp. 401–420.

[28] H.-D. Tran, D. M. Lopez, P. Musau, X. Yang, L. V. Nguyen, W. Xiang, and T. T. Johnson, "Star-based reachability analysis of deep neural networks," in *International Symposium on Formal Methods*, Springer, 2019, pp. 670–686.

[29] I. M. Mitchell, A. M. Bayen, and C. J. Tomlin, "A time-dependent Hamilton-Jacobi formulation of reachable sets for continuous dynamic games," *IEEE Transactions on automatic control*, vol. 50, no. 7, pp. 947–957, 2005.

[30] I. M. Mitchell, "A toolbox of level set methods," *UBC Department of Computer Science Technical Report TR-2007-11*, 2007.

[31] J. B. Lasserre, *Moments, positive polynomials and their applications*. World Scientific, 2009, vol. 1.

[32] A. Majumdar, R. Vasudevan, M. M. Tobenkin, and R. Tedrake, "Convex optimization of nonlinear feedback controllers via occupation measures," *The International Journal of Robotics Research*, vol. 33, no. 9, pp. 1209–1230, 2014.

[33] P. Holmes, S. Kousik, S. Mohan, and R. Vasudevan, "Convex estimation of the α -confidence reachable set for systems with parametric uncertainty," in *2016 IEEE 55th Conference on Decision and Control (CDC)*, IEEE, 2016, pp. 4097–4103.

[34] A. A. Requicha and H. B. Voelcker, "Constructive solid geometry," 1977.

[35] J. D. Foley, F. D. Van, A. Van Dam, S. K. Feiner, J. F. Hughes, E. Angel, and J. Hughes, *Computer graphics: principles and practice*. Addison-Wesley Professional, 1996, vol. 12110.

[36] M. Lutz and T. Meurer, *Efficient formulation of collision avoidance constraints in optimization based trajectory planning and control*, 2021.

- [37] I. M. Mitchell, M. Chen, and M. Oishi, "Ensuring safety of nonlinear sampled data systems through reachability (extended version)," Technical Report TR-2012-01, Department of Computer Science, University of California, Berkeley, Tech. Rep., 2012.
- [38] V. Gaßmann and M. Althoff, "Scalable Zonotope-Ellipsoid Conversions using the Euclidean Zonotope Norm," in *2020 American Control Conference (ACC)*, IEEE, 2020, pp. 4715–4721.
- [39] S. Kousik, P. Holmes, and R. Vasudevan, "Safe, aggressive quadrotor flight via reachability-based trajectory design," in *Dynamic Systems and Control Conference*, American Society of Mechanical Engineers, vol. 59162, 2019, V003T19A010.
- [40] V. Macagon and B. Wünsche, "Efficient collision detection for skeletally animated models in interactive environments," *Proceedings of IVCNZ'03*, pp. 378–383, 2003.
- [41] C. Liu and M. Tomizuka, "Algorithmic safety measures for intelligent industrial co-robots," in *2016 IEEE International Conference on Robotics and Automation (ICRA)*, IEEE, 2016, pp. 3095–3102.
- [42] M. Althoff, "An introduction to cora 2015," in *Proc. of the Workshop on Applied Verification for Continuous and Hybrid Systems*, 2015.
- [43] A. Bry and N. Roy, "Rapidly-exploring random belief trees for motion planning under uncertainty," in *2011 IEEE international conference on robotics and automation*, IEEE, 2011, pp. 723–730.
- [44] U. Malik, I. M. Jaimoukha, G. D. Halikias, and S. Gungah, "On the gap between the quadratic integer programming problem and its semidefinite relaxation," *Mathematical programming*, vol. 107, no. 3, pp. 505–515, 2006.

APPENDIX

A. Ellipsoid Visualization

Zonotopes in general can be difficult to visualize due to the exponential number of faces as a function of the number of generators. Ellipsotopes are further challenging because we are now concerned with plotting an affine image of, in the most general sense, the intersection of a hyperplane with a Cartesian product of high-dimensional p -norm balls. We now describe several "tricks" to facilitate visualization.

For this appendix, consider $c \in \mathbb{R}^n$, $G \in \mathbb{R}^{n \times m}$, $A \in \mathbb{R}^{k \times m}$, and $b \in \mathbb{R}^k$; and, let \mathcal{J} be a valid index set.

1) *High-dimensional Ball Boundaries*: The first trick that we leverage is that, since an ellipsoid is an affine image of a convex shape in high dimensions, the boundary of the image is a subset of the image of the boundary. Consequently, our strategy for visualization is to generate points on the *boundary* of the feasible generator coefficients, then map them through the generator matrix. While many of these points may not lay on the boundary of the ellipsoid, the convex hull of these points is a visually-acceptable approximation of the ellipsoid in practice.

To proceed, we first need the following lemma.

Lemma 15. *Suppose $C \in \mathbb{R}^n$ is a compact, convex set. Let $M : \mathbb{R}^n \rightarrow \mathbb{R}^m$ with $m < n$ be a surjective linear map. Suppose $x \in \text{bd}(MC)$. Then there exists $y \in \text{bd}(C)$ such that $x = My$.*

Proof. The preimage $M^{-1}x$ is a linear subspace of \mathbb{R}^n that intersects C , and therefore intersects $\text{bd}(C)$. \square

Now, to approximate the boundary of a high-dimensional ball, suppose that $Y \subset \mathbb{R}^n$ is a finite set of sampled points with $|Y| = n_{\text{plot}} \in \mathbb{N}$. To map $Y \rightarrow \text{bd}(\mathcal{B}_{p,n})$, let $\text{bdproj}_p(\cdot) : \mathbb{R}^n \rightarrow \mathbb{R}^n$ for which

$$\text{bdproj}_p(y) = \frac{y \langle i \rangle}{\|y \langle i \rangle\|_p}. \quad (39)$$

Suppose $E = \mathcal{E}_p(c, G)$. Let $X = c + G \cdot \text{bdproj}_p(Y)$. Then, applying Lemma 15, $\text{CH}(X)$ approximates E , where $\text{CH}(\cdot)$ returns the convex hull of a set.

2) *Ball Product and Affine Subspace Ray Tracing*: Now we generalize the previous approach to generate points on the boundary of the intersection of the ball product $\mathcal{B}_\times(\mathcal{J})$ and the affine subspace $\mathcal{P}(A, b)$. Let $E = \mathcal{E}_p(c, G, A, b, \mathcal{J})$. To plot this ellipsoid, our goal is to first pick $n_{\text{plot}} \in \mathbb{N}$ coefficients β_i , $i = 1, \dots, n_{\text{plot}}$, such that

$$\beta_i \in \text{bd}(\mathcal{B}_\times(\mathcal{J}) \cap \mathcal{P}(A, b)). \quad (40)$$

In other words, these coefficients obey the constraints

$$\forall J \in \mathcal{J}, \|\beta_i \langle J \rangle\|_p \leq 1, \quad (41a)$$

$$\exists K \in \mathcal{J} \text{ s.t. } \|\beta_i \langle K \rangle\|_p = 1, \text{ and} \quad (41b)$$

$$A\beta = b. \quad (41c)$$

We can then approximate the ellipsoid as

$$E \approx \text{CH}\left(\{c + G\beta_i\}_{i=1}^{n_{\text{plot}}}\right). \quad (42)$$

We generate these points by tracing rays outwards in \mathbb{R}^m from a point inside $\mathcal{B}_\times(\mathcal{J})$ until they contact the boundary of $\mathcal{B}_\times(\mathcal{J}) \cap \mathcal{P}(A, b)$.

To generate a single β_i , first let $u_i \in \ker(A)$ be a random vector in the nullspace of A . Let $\beta_0 \in \mathcal{B}_\times(\mathcal{J})$, which can be found by applying Corollary 8; note that $\beta_0 = A^\dagger b$ is often such a point. Let $J \in \mathcal{J}$. We then solve

$$\|\alpha_i u_i \langle J \rangle + \beta_0 \langle J \rangle\|_p = 1 \quad (43)$$

for $\alpha_i \in \mathbb{R}$ and set $\beta_i = \alpha_i u_i + \beta_0$ as a point that is guaranteed to obey (41). Let $\varphi(\alpha_i, u_i, \beta_0, J) = \|\alpha_i u_i \langle J \rangle + \beta_0 \langle J \rangle\|_p^p - 1^p$. Notice that, for any $J \in \mathcal{J}$,

$$\begin{aligned} \varphi(\alpha_i, u_i, \beta_0, J) &= \left(\sum_{j \in \mathcal{J}} ((\alpha_i u_i \langle j \rangle)^p + (\beta_0 \langle j \rangle)^p) \right) - 1 \quad (44) \\ &= \binom{p}{0} \alpha_i^p \sum_{j \in \mathcal{J}} (u_i \langle j \rangle)^p (\beta_0 \langle j \rangle)^0 + \\ &\quad + \binom{p}{1} \alpha_i^{p-1} \sum_{j \in \mathcal{J}} (u_i \langle j \rangle)^{p-1} (\beta_0 \langle j \rangle)^1 + \dots \\ &\quad \dots + \binom{p}{p} \alpha_i^0 \sum_{j \in \mathcal{J}} (u_i \langle j \rangle)^0 (\beta_0 \langle j \rangle)^p - 1, \end{aligned} \quad (45)$$

where we have applied the binomial theorem to expand the coefficients. Since $\varphi(\cdot, u_i, t, J)$ is a univariate polynomial in α_i , we can solve for α_i efficiently. Critically, since $\beta_0 \in \mathcal{B}_\times(\mathcal{J})$, the direction u_i points "outward" towards the boundary, so the smallest solution α_i is a point on the boundary; in other words, β_i obeys (41).

3) *Ray Tracing*: We find in practice that plotting 2-D ellipsotopes with more than 5 generators with the above methods is computationally expensive, taking several seconds to generate a single plot. Furthermore, the above methods result in many unused points (that is, points on the boundary of the feasible set that are mapped to the interior of the ellipsoid, and therefore not used for plotting). To address

this, we pose a convex program to identify points on the boundary of the ellipsotope directly in its workspace. In particular, we maximize the length of a ray extending from a point in the ellipsotope in an arbitrary direction while constraining it to lie within the ellipsotope.

We set up for ray tracing as follows. Let $E = \mathcal{E}_p(c, G, A, B, \mathcal{J}) \subset \mathbb{R}^n$ be an ellipsotope with m generators. Consider a ray

$$\mathcal{R}(x, g) = \{x + \lambda g \mid \lambda \geq 0\} \subset \mathbb{R}^n, \quad (46)$$

where $g \in \mathbb{R}^n$ is arbitrary and $x \in E$. We find x as any feasible point in the ellipsotope by applying the strategy above in Appendix A.2 to find a feasible coefficient β , then setting $x = c + G\beta$. Note, we cannot always set $x = c$, because it is possible that $c \notin E$, which occurs when $0 \notin \mathcal{P}(A, b)$.

Finally, to perform ray tracing, we solve

$$\max_{\lambda \geq 0, \beta \in \mathbb{R}^m} \lambda \quad (47a)$$

$$\text{s.t.} \quad \|\beta \langle J \rangle\|_p \leq 1 \quad \forall J \in \mathcal{J}, \quad (47b)$$

$$A\beta = b, \text{ and} \quad (47c)$$

$$c + G\beta = x + \lambda g, \quad (47d)$$

which is convex and always feasible if $E \neq \emptyset$. By solving (47) for a variety of g , we can sample the boundary of the ellipsotope. In practice, we sample g uniformly from the boundary of the 2-D or 3-D unit sphere and solve (47) once for each sample.

B. Minimum Volume Outer Ellipsoids

We use the following methods to compute minimum volume outer ellipsoids (MVOEs) for the Minkowski sum of ellipsoids and for zonotopes. These objects are useful for order reduction as discussed in Section V.

1) *MVOE of Ellipsoid Minkowski Sum*: We apply the method in [14]. Consider the pair of ellipsoids $E_1 = \mathcal{E}(c_1, Q_1)$ and $E_2 = \mathcal{E}(c_2, Q_2)$ in \mathbb{R}^n . Let $\lambda = \text{eig}(Q_1 Q_2^{-1}) \in \mathbb{R}^n$. Let $\zeta_0 \in \mathbb{R}$ and consider the fixed-point iteration

$$\zeta_{n+1} = \left(\frac{\sum_{i=1}^n \frac{1}{1 + \zeta_n \lambda \langle i \rangle}}{\sum_{i=1}^n \frac{\lambda \langle i \rangle}{1 + \zeta_n \lambda \langle i \rangle}} \right)^{\frac{1}{2}}. \quad (48)$$

Define ζ as the limit of (48) as $n \rightarrow \infty$. Then

$$E_1 \oplus E_2 \subseteq \mathcal{E}(c_1 + c_2, Q_{\oplus}), \quad (49)$$

where

$$Q_{\oplus} = \left(\left(1 + \frac{1}{\zeta}\right) Q_1^{-1} + (1 + \zeta) Q_2^{-1} \right)^{-1}. \quad (50)$$

See [14, Sec. III-B and Sec. IV-B] for derivation and analysis of the above algorithm, and in particular [14, Thm. 1] for a proof of convergence.

We find ζ numerically by applying [14, (17)]. First, we set a tolerance $\varepsilon \approx 10^{-10}$. Then, we iterate (48) starting from $\zeta_0 = 0$ until

$$\sum_{i=1}^n \frac{1 - \zeta^2 \lambda \langle i \rangle}{1 + \zeta \lambda \langle i \rangle} \leq \varepsilon. \quad (51)$$

2) *Overapproximating the MVOE of a Zonotope*: We apply the method in [38, Thm. 1]. Let $Z = \mathcal{Z}(c, G) \subset \mathbb{R}^n$ be a zonotope with $m \in \mathbb{N}$ generators. To overapproximate the MVOE, we first solve an SDP [38, Lem. 3]:

$$r = \min_{\lambda \geq 0, \lambda \in \mathbb{R}^m} \mathbf{1}_{m \times 1}^\top \lambda \quad (52)$$

$$\text{s.t.} \quad \text{diag}(\lambda) - G_0^\top G_0 \succeq 0, \quad (53)$$

where

$$G_0 = E_0^{-\frac{1}{2}} \quad \text{and} \quad E_0 = mGG^\top. \quad (54)$$

Then an outer approximation of the MVOE is given by

$$Z \subset \mathcal{E}(c, rE_0). \quad (55)$$

The MVOE approximation can be made tighter by applying [44, Lem. 3] in the case when $n \approx m$.